https://doi.org/10.1016/j.bone.2017.01.029

Elsevier Editorial System(tm) for Bone
Manuscript Draft

Manuscript Number: BONE-D-16-00633R2

Title: Differential response of bone and kidney to ACEI in db/db mice: A potential effect of captopril on accelerating bone loss

Article Type: Full length article

Keywords: Diabetes; Bone; Kidney; Osteoporosis; Captopril; Renin-angiotensin system

Corresponding Author: Professor Yan Zhang, Ph.D

Corresponding Author's Institution: Longhua Hospital, Shanghai University of Traditional Chinese Medicine

First Author: Yan Zhang, Ph.D

Order of Authors: Yan Zhang, Ph.D; Xiao-Li Li, Ph.D; Nan-Nan Sha; Bing Shu, Ph.D; Yong-Jian Zhao; Xin-Luan Wang, Ph.D; Hui-Hui Xiao, Ph.D; Qi Shi, M.D; Man-Sau Wong, Ph.D; Yong-Jun Wang, M.D., Ph.D

Abstract: The components of renin-angiotensin system (RAS) are expressed in the kidney and bone. Kidney disease and bone injury are common complications associated with diabetes. This study aimed to investigate the effects of an angiotensin-converting enzyme inhibitor, captopril, on the kidney and bone of db/db mice. The db/db mice were orally administered by gavage with captopril for 8 weeks with db/+ mice as the non-diabetic control. Serum and urine biochemistries were determined by standard colorimetric methods or ELISA. Histological measurements were performed on the kidney by periodic acid-schiff staining and on the tibial proximal metaphysis by safranin O and masson-trichrome staining. Trabecular bone mass and bone quality were analyzed by microcomputed tomography. Quantitative polymerase chain reaction and immunoblotting were applied for molecular analysis on mRNA and protein expression. Captopril significantly improved albuminuria and glomerulosclerosis in db/db mice, and these effects might be attributed to the down-regulation of angiotensin II expression and the expression of its down-stream profibrotic factors in the kidney, like connective tissue growth factor and vascular endothelial growth factor. Urinary excretion of calcium and phosphorus markedly increased in db/db mice in response to captopril. Treatment with captopril induced a decrease in bone mineral density and deterioration of trabecular bone at proximal metaphysis of tibia in db/db mice, as shown in the histological and reconstructed 3-dimensional images. Even though captopril effectively reversed the diabetes-induced changes in calcium-binding protein 28-k and vitamin D receptor expression in the kidney as well as the expression of RAS components and bradykinin receptor-2 in bone tissue, treatment with captopril increased the osteoclast-covered bone surface, reduced the osteoblast-covered bone surface, down-regulated the expression of type 1 collagen and transcription factor runt-related transcription factor 2 (markers for osteoblastic functions), and up-regulated the expression of carbonic anhydrase II (marker for bone resorption). Captopril exerted therapeutic effects on renal injuries associated with type 2 diabetes but worsened the deteriorations of trabecular bone in db/db mice; the latter of which

was at least in part due to the stimulation of osteoclastogenesis and the suppression of osteogenesis by captopril.

***Highlights (for review)**

1. Captopril improved diabetic nephropathy by suppressing the expression of ANG II and profibrotic factors in kidney of db/db mice.
2. Treatment with Captopril induced the decrease of bone mineral density and the deteriorations of trabecular bone in db/db mice.
3. Captopril inhibited the expression of RAS components in kidney and bone of type 2 diabetic mice.
4. Captopril worsened the deteriorations of trabecular bone by stimulating osteoclastogenesis and suppressing osteogenesis.

Differential response of bone and kidney to ACEI in db/db mice: A potential effect of captopril on accelerating bone loss

Yan Zhang[1*], Xiao-Li Li[2], Nan-Nan Sha[1], Bing Shu[1], Yong-Jian Zhao[1], Xin-Luan Wang[3], Hui-Hui Xiao[4,5], Qi Shi[1], Man-Sau Wong[5], Yong-Jun Wang[1,6*]

1. Spine Disease Research Institute, Longhua Hospital, Shanghai University of Traditional Chinese Medicine, Shanghai 200032, China

2. School of Medical Instrument and Food Engineering, University of Shanghai for Science and Technology, Shanghai 200093, China

3. Translational Medicine R&D Center, Institute of Biomedical and Health Engineering, Shenzhen Institutes of Advanced Technology, Chinese Academy of Sciences, Shenzhen 518055, China

4. State Key Laboratory of Chinese Medicine and Molecular Pharmacology (Incubation), Shenzhen Research Institute of The Hong Kong Polytechnic University, Shenzhen 518057, China

5. Department of Applied Biology and Chemical Technology, The Hong Kong Polytechnic University, Hung Hom, Kowloon, Hong Kong SAR, China

6. School of Rehabilitation Science, Shanghai University of Traditional Chinese Medicine, Shanghai 201203, China

* Corresponding author: Prof. Yan Zhang & Prof. Yong-Jun Wang

Yan Zhang, Ph.D

E-mail: medicineyan@163.com

Tel: (86)21-64385700-9905 ; Fax: (86)21-64398310

Yong-Jun Wang, M.D

E-mail: yjwang8888@126.com

Tel: (86)21-64385811; Fax: (86)21-64398310

Abstract

The components of renin-angiotensin system (RAS) are expressed in the kidney and bone. Kidney disease and bone injury are common complications associated with diabetes. This study aimed to investigate the effects of an angiotensin-converting enzyme inhibitor, captopril, on the kidney and bone of db/db mice. The db/db mice were orally administered by gavage with captopril for 8 weeks with db/+ mice as the non-diabetic control. Serum and urine biochemistries were determined by standard colorimetric methods or ELISA. Histological measurements were performed on the kidney by periodic acid-schiff staining and on the tibial proximal metaphysis by safranin O and masson-trichrome staining. Trabecular bone mass and bone quality were analyzed by microcomputed tomography. Quantitative polymerase chain reaction and immunoblotting were applied for molecular analysis on mRNA and protein expression. Captopril significantly improved albuminuria and glomerulosclerosis in db/db mice, and these effects might be attributed to the down-regulation of angiotensin II expression and the expression of its down-stream profibrotic factors in the kidney, like connective tissue growth factor and vascular endothelial growth factor. Urinary excretion of calcium and phosphorus markedly increased in db/db mice in response to captopril. Treatment with captopril induced a decrease in bone mineral density and deterioration of trabecular bone at proximal metaphysis of tibia in db/db mice, as shown in the histological and reconstructed 3-dimensional images. Even though captopril effectively reversed the diabetes-induced changes in calcium-binding protein 28-k and vitamin D receptor

expression in the kidney as well as the expression of RAS components and bradykinin receptor-2 in bone tissue, treatment with captopril increased the osteoclast-covered bone surface, reduced the osteoblast-covered bone surface, down-regulated the expression of type 1 collagen and transcription factor runt-related transcription factor 2 (markers for osteoblastic functions), and up-regulated the expression of carbonic anhydrase II (marker for bone resorption). Captopril exerted therapeutic effects on renal injuries associated with type 2 diabetes but worsened the deteriorations of trabecular bone in db/db mice; the latter of which was at least in part due to the stimulation of osteoclastogenesis and the suppression of osteogenesis by captopril.

Keywords: Diabetes, Bone, Kidney, Osteoporosis, Captopril, Renin-angiotensin system

Introduction

The renin-angiotensin system (RAS) is a hormonal cascade that is thought to play a key role in regulating blood pressure as well as fluid balance within the body [1]. Angiotensinogen (AGT) secreted by the liver is enzymatically cleaved to angiotensin (ANG) I by kidney-derived renin. ANG I is hereafter cleaved by angiotensin-converting enzyme (ACE) to the effector hormone ANG II [2]. However, this classical theory has been fundamentally revised in recent years. It is now evident that the components of RAS, in addition to the classical pathway, are produced and act locally in multiple tissues, a concept known as tissue RAS [3].

The local effects of tissue RAS are diverse and depend on the specific tissues involved. It is well established that an activated RAS is a major risk factor of both cardiovascular and renal diseases [4-7]. The inhibitors of RAS [ACE inhibitors (ACEI), ANG II receptor blockers (ARB), and renin inhibitors] are therefore widely used in clinic. With the demonstration of the biological effects of ANG II on bone tissue [8] and the expression of RAS components in bone tissue and primary culturing bone cells [9, 10], the key role that skeletal RAS plays in regulating bone metabolism has been progressively revealed. Previously, most of the clinical studies showed that patients treated with ACEI showed an increased bone mineral density (BMD) and a reduced fracture risk [11-16]. However, recently emerging evidences indicated that the use of ACEI did not change the rate or the risk of fracture [17]; it even led to greater bone loss [18-20]. Thus, the findings from previous clinical investigations were inconsistent about the effects of ACEI on bone.

The world prevalence of diabetes among adults (aged 20–79 years) was 6.4%, affecting 285 million of adults in 2010, and it will increase to 7.7%, and 439 million of adults by 2030 [21]. Under chronic condition diabetes mellitus (DM) adversely affects different parts of the body, including bone, nerve, muscles, retina of the eyes, the cardiovascular system and the nephron of kidney [22]. Animal studies in our group demonstrated that the increase in activity of skeletal RAS was involved in the pathological process of type 1 diabetes-induced osteoporosis [23, 24], while the RAS inhibitors, including ACEI [24] and ARB [23], did not effectively reverse bone injuries in type 1 diabetic mice model. In addition, our studies revealed that losartan (which belongs to ARB) and aliskiren (a renin inhibitor) improved the development of nephropathy associated with type 1 diabetes [4, 5, 25], which is the most common renal complication of DM and a leading cause of end-stage renal disease. Thus, given that type 2 diabetes is much more prevalent in humans than type 1 diabetes, we are keen to know the potential effects of ACEI on the kidney and bone in type 2 diabetic animal models.

Herein we reported the results about the effects of captopril, one of the ACEIs, on renal disease and osteoporosis that were associated with type 2 diabetes as well as the modulation of tissue RAS and other pathological molecules by captopril in the kidney and bone of db/db mice, a commonly used type 2 diabetic animal model. The present study demonstrated the protective effects of captopril against type 2 diabetic nephropathy and the impairing effects of captopril on skeletal tissue of db/db mice.

Materials and methods

Animals and treatment

$Lpr^{db/db}$ (db/db) and $Lpr^{db/+}$ (db/+) mice in C57BL/6-KS background were purchased from Slac Laboratory (Shanghai, China). The animals were housed in environmentally controlled central animal facilities, and kept in 22°C, light : dark (12 h : 12 h) conditions and fed with commercial diet and distilled water *ad libitum* during the experimental period. Six-month-old male db/db mice were randomized into diabetes group (n = 12) and captopril-treated group (n = 12). The db/+ mice served as the non-diabetic control (n = 10). The mice were orally administered with captopril at a single dosage of 10 mg/kg by gavage or with distilled water as vehicle daily. Body weight and fasting blood glucose monitoring were performed monthly. Eight weeks after drug administration, spot urine of each mouse was collected. Serum, kidneys, tibias and femurs were immediately harvested for a variety of biochemical, histological and molecular analyses. The animal study protocol was reviewed and approved by the Animal Ethics Committee of Shanghai University of Traditional Chinese Medicine. The methods were carried out in accordance with the *Guide for the Care and Use of Laboratory Animals* (8^{th} edition, Institute of Laboratory Animal Resources on Life Sciences, National Research Council, National Academy of Sciences, Washington DC).

Serum and urine chemistry

Calcium (Ca), phosphorus (P) and creatinine (Cr) concentrations in serum and urine were measured by standard colorimetric methods using a micro-plate reader (Bio-Tek,

USA). The level of urine Ca and P was corrected by the concentration of urine Cr. Serum levels of intact parathyroid hormone (PTH) and fibroblast growth factor-23 (FGF-23) were determined using mouse bioactive PTH and FGF-23 (C-Term) ELISA assay (Immutopics, Inc., San Clemente, CA, USA). The kit for serum testosterone was provided by ALPCO (USA). Urinary albumin level was determined using commercial kits as reported previously [26].

Histological staining on bone

The tibias were fixed in 4% formaldehyde/PBS (pH 7.2), decalcified in 0.5 M EDTA (pH 8.0), and embedded in paraffin by standard histological procedures. Serial sections of 3 μm were cut. The tibial proximal metaphysis was the region of interest. Safranin O (Sigma-Aldrich) staining was performed together with fast green and counter stain by hematoxylin. The masson-trichrome staining was also performed. Trabecular bone quantity expressed as trabecular bone area over total area (BA/TA) was measured using the OsteoMeasure system (OsteoMetrics Inc., Decatur, GA, USA). The thickness of the cartilage overlying growth plate was measured by blind assessment for 10 different sites of each slide using LAS v3.6 software coupled with a microscope (Leica DM 2500, Germany). Additionally, tartrate-resistant acid phosphatase (TRAP) and modified Gomori stainings were used for the identification of osteoclasts and osteoblasts, respectively, following the manufacturer's instructions (Sigma, St Louis, USA and Yuanmu Biotechnology, Shanghai, China). The osteoclast-covered bone surface (OcS/BS) and osteoblast-covered bone surface (ObS/BS) were also determined by the OsteoMeasure system. Stained slides were

visualized under microscope.

PAS staining on kidney

Freshly dissected kidneys were fixed overnight with 4% formaldehyde in phosphate-buffered saline (pH 7.2), processed, embedded in paraffin, and cut into 3-μm sections. Renal sections were stained with periodic acid-Schiff (PAS). Semi-quantitative scoring of glomerular sclerosis in PAS-stained slides was performed in a blinded fashion by a renal pathologist (AC) using a five-grade method as described previously [26]: 0, normal glomerulus; 1, sclerosis <25% of glomerular surface; 2, sclerosis between 25 and 50%; 3, sclerosis between 50 and 75%; and 4, sclerosis >75% of glomerular surface.

Micro-CT analysis

The tibia of each animal was scanned to obtain three-dimensional (3D) images and quantitative parameters of trabecular bone at the proximal metaphysis of tibia. The detection process and the setting of relevant detecting parameters were as described previously [24]. Briefly, the proximal tibial metaphysis underneath the growth plate was examined on 1.81 mm slab, corresponding to 173 slices, with a high-resolution micro viva-CT40 system (Scanco Medical, Bassersdorf, Switzerland). The scanning parameters used were 70 kVp, 111 μA, and 1000 projections per 180°, resulting in a 10.5 μm isotropic voxel size and a total scan time of 13.2 minutes. Hand-drawn contours were used to isolate the metaphyseal region of interest and trabecular compartments based on 100 consecutive slices. Trabecular bone micro-architecture was assessed using the μCT Evaluation Program (Image Processing Language v. 5.0A,

Scanco). The 3D parameters for trabecular bone were obtained as follows: (1) bone volume over total volume (BV/TV); (2) connectivity density (Conn.D); (3) structure model index (SMI); (4) trabecular bone number (Tb.N); (5) trabecular bone thickness (Tb.Th); (6) trabecular bone separation (Tb.Sp); (7) the mean mineral density of total volume (BMD/TV); (8) bone surface over bone volume (BS/BV); (9) the geometric degree of anisotropy (DA).

RT-PCR and quantitative RT-PCR

Total tissue RNA was isolated according to the TRIzol manufacturer's protocol (Invitrogen, Carlsbad, California, USA). Synthesis of cDNAs was performed by reverse transcription reactions with 4 μg of total RNA using moloney murine leukemia virus reverse transcriptase (Invitrogen, Carlsbad, California, USA) with oligo $dT_{(15)}$ primers (Fermentas). The first strand cDNAs served as the template for the regular PCR performed using a DNA Engine (ABI), or for quantitative PCR performed in Applied Biosystems 7900 Real Time PCR System using a SYBR green PCR reagent kit (Applied Biosystems, Foster City, CA, USA). Glyceraldehyde-3-phosphate dehydrogenase (*GAPDH*) as an internal control was used to normalize the data to determine the relative expression of the target genes. The PCR primers used in this study were as previously described [4, 27, 28].

Western blotting

The proteins were extracted in Laemmli buffer (Boston Bioproducts, Worcester, MA, USA). Samples containing 40 μg of protein were separated on 10% SDS-PAGE gel, and transferred to nitrocellulose membranes (Whatman). After saturation with 5%

(w/v) nonfat dry milk in TBS and 0.1% (w/v) Tween 20 (TBST), the membranes were incubated with primary antibodies, purchased from Santa Cruz Biotechnology (USA), at dilutions ranging from 1:1000 to 1:2000 at 4°C overnight. After three washes with TBST, membranes were incubated with secondary immunoglobulins conjugated to IRDye 800CW Infrared Dye (LI-COR), including donkey anti-goat IgG and donkey anti-mouse IgG at the dilution of 1:15000. Blots were visualized by the Odyssey Infrared Imaging System (LI-COR Biotechnology, USA). Signals were densitometrically assessed (Odyssey Application Software version 3.0) and normalized to the β-actin signals to correct for unequal loading using the mouse monoclonal anti-β-actin antibody (Sigma, USA).

Statistical analysis

The data from these experiments were reported as mean ± standard error of mean (SEM) for each group. All statistical analyses were performed using PRISM version 4.0 (GraphPad). Inter-group differences were analyzed by one-way ANOVA, followed by Tukey's multiple comparison test as a post test to compare the group means if overall $P < 0.05$. Differences with P value of less than 0.05 were considered statistically significant.

Results

Physiological markers

As expected, the baseline body weight (Fig. 1A) and fasting blood glucose level (Fig. 1B) of the db/db mice were much higher ($P < 0.001$) than those of db/+ mice, and age had little effect on the fasting blood glucose level of the db/+ mice. The captopril treatment had no effects on the body weight and blood glucose level of these mice (Fig. 1). Therefore, the effect resulting from the drug treatment is unlikely to be mediated through targeting the pancreas or by reducing hyperglycemia.

Biochemical markers in serum and urine

The serum creatinine level was elevated (Fig. 1C, $P < 0.05$) in vehicle-treated db/db mice, which was significantly reduced ($P < 0.05$) by captopril treatment. There were no statistical differences in the calcium and phosphorus in serum and urine between the non-diabetic and diabetic mice (Table 1). However, captopril treatment significantly elevated ($P < 0.05$) urine calcium and phosphorus levels of the db/db mice.

Serum parathyroid hormone (PTH) level was elevated (Table 2, $P < 0.05$) and serum fibroblast growth factor-23 (FGF-23) level was reduced ($P < 0.01$) in db/db mice. Treatment of db/db mice with captopril almost completely prevented the increase in serum PTH, whose value was maintained at a level similar to that of nondiabetic mice, while serum testosterone and FGF-23 levels in db/db mice were not altered by the treatment.

The diabetic mice in the db/db group developed albuminuria (Fig. 1D), and the urinary albumin-to-creatinine ratio (ACR) increased by more than twofold ($P < 0.001$) over that of the non-diabetic mice. Captopril had significant inhibitory effect ($P < 0.01$) on the development of albuminuria in db/db mice upon treatment for 8 weeks. Therefore, the therapy with captopril markedly prevented the development of proteinuria in the diabetic animals.

Glomerulosclerosis

Glomerular sclerosis is an important feature of hyperglycemia-induced renal injury. PAS staining and semiquantitative scoring were used to assess the degree of glomerulosclerosis in the kidney. Compared with the control mice, diabetic mice showed marked glomerulosclerosis (Fig. 2A), which was reduced by captopril treatment (Fig. 2A). A semiquantitative glomerulosclerotic index of kidney sections confirmed the histological data. The diabetic mice in db/db group showed the highest score (Fig. 2B, $P < 0.01$), and treatment with captopril led to a significant reduction in the index ($P < 0.05$) in db/db mice as compared to db/db mice treated with vehicle.

Expression of angiotensin II and profibrotic factors in the kidney

Angiotensin II (ANG II) is the active peptide in the renin-angiotensin system (RAS) and regulates the downstream effectors, including profibrotic cytokines, which mediate renal injury. The effects of captopril on the expression of ANG II, connective tissue growth factor (*CTGF*), vascular endothelial growth factor (*VEGF*) in the kidney

(Fig. 2C-F) were measured, and these factors were known to be involved in the development of diabetic renal damage. The vehicle-treated diabetic mice showed robust increase in ANG II (Fig. 2D, $P < 0.01$), *CTGF* (Fig. 2F, $P < 0.001$) and *VEGF* ($P < 0.05$) in comparison to those of the nondiabetic control. The induction of these factors was suppressed by the treatment with captopril (Fig. 2, D and F, $P < 0.05$).

Histology of proximal tibial metaphysis

Safranin O staining (Fig. 3A) and Masson-Trichrome staining (Fig. 3B) were conducted to evaluate the effects of treatment on the epiphyseal region of proximal tibial metaphysis. The loss of bone quantity and network connection of trabecular bone was clearly shown at the secondary spongiosa zone of proximal tibia in the diabetic group as compared with the normal control group (Fig. 3C, $P < 0.01$). Similarly, the thickness of the cartilages overlying the epiphyseal plate in the diabetic group was reduced (Fig. 3D, $P < 0.05$), suggesting the occurrence of delayed formation of new cartilages. Treatment with captopril did not improve the pathological alterations of proximal metaphysis of tibia in the diabetic mice, and even led to more decrease in BA/TA (Fig. 3C, $P < 0.01$) than that in the db/db group. Thus, the histological stainings revealed that captopril did not reverse the remarkable abnormalities of trabecular bone at the proximal tibial metaphysis of the diabetic mice.

Micro CT analysis

To quantitatively evaluate the effects of captopril on trabecular bone of diabetic mice, 3D micro-computed tomography was performed on the proximal metaphysis of tibia. The profiles of 3D images (Fig. 4) clearly demonstrated a loss of trabecular bone mass and trabecular bone number at the proximal metaphysis of tibia of the db/db mice, and the 3D bone biological parameters (Table. 3) quantitatively reflected these observed changes. Diabetes induced a marked decrease ($P < 0.01$) in BV/TV, Conn.D, Tb.N, Tb.Th, and BMD/TV, and an increase ($P < 0.05$) in SMI, Tb.Sp and BS/BV in the db/db mice. Moreover, captopril treatment further significantly reduced BV/TV ($P < 0.01$), Tb.N ($P < 0.001$) and BMD/TV ($P < 0.01$) and induced Tb.Sp ($P < 0.01$) in the db/db mice as compared with those of the vehicle-treated diabetic mice.

Expression of RAS components in femur

The mRNA (Fig. 5) and protein (Fig. 6) expressions of RAS components, including renin, angiotensin II (ANG II), ANG II type 1 receptor (AT1R), renin receptor (Renin-R), bradykinin B1 receptor (B1R) and B2 receptor (B2R), were measured in the femur of the mice. The expression of these proteins in femur of the diabetic mice, except that of B1R, was all significantly up-regulated in comparison with those of the non-diabetic control. Treatment with captopril dramatically down-regulated the mRNA expression of *renin* ($P < 0.01$), *Renin-R* ($P < 0.05$) and *AT1R* ($P < 0.05$), and decreased the protein expression of renin ($P < 0.01$), ANG II ($P < 0.01$) and B2R ($P < 0.05$) in the db/db mice as compared with those of the diabetic mice, suggesting the potential suppressive action of captopril on the bone tissue RAS of the db/db mice.

Histological stainings for osteoclasts and osteoblasts

In the normal control group, few osteoclasts could be identified in the trabecular bone area underneath the growth plate of the proximal tibial metaphysis (Fig. 7A, shown by blue arrow). In contrast, TRAP-positive matured osteoclasts were found in this bone site of the db/db mice and the number of osteoclasts was significantly increased in the captopril-treated db/db mice. Such observation was consistent with the fact that treatment of the db/db mice with captopril enhanced the osteoclast-covered bone surface (OcS/BS) as compared with that of the db/db mice ($P < 0.05$, Fig. 7B).

Modified Gomori staining was used to detect alkaline phosphatase activity for indicating osteoblasts in the proximal metaphysis of tibia. The value for osteoblast-covered bone surface (ObS/BS) was obtained based on the positive staining with black color (Fig. 7C). A significant decrease in ObS/BS ($P < 0.05$, Fig. 7D) was shown in the db/db group as compared with the db/+ group, and it was further reduced in the captopril-treated db/db mice ($P < 0.05$).

mRNA expression of key regulators for bone metabolism

As the balance of bone metabolism was directly regulated by the activities of bone formation and bone resorption, measurement of the expression of osteoblast- (*COL*, *RUNX2*) and osteoclast-specific (*CAII*, *MMP-9*) genes was performed (Fig. 8A & B). As expected, the db/db mice showed a lower expression ($P < 0.05$) of *COL* and

RUNX2 and a higher expression ($P < 0.05$) of *CAII* and *MMP-9* than those of the normal control group. Interestingly, captopril induced further down-regulation ($P < 0.01$) of *COL* and *RUNX2* and up-regulation ($P < 0.05$) of *CAII* in the db/db mice as compared with those of the diabetic mice.

Expression of calcium metabolism regulators in kidney

Calcium homeostasis plays a vital role in maintaining bone health, thus, the expression of key regulators which are responsible for handling calcium metabolism in kidney was determined (Fig. 9). In the vehicle-treated diabetic mice, chronic hyperglycemia caused a marked increase ($P < 0.01$) in the protein expression of calcium-binding protein 28k (CaBP-28k) and a significant decrease ($P < 0.001$) in the protein expression of vitamin D receptor (VDR) of the kidney. The alterations of these factors were inhibited by the treatment with captopril ($P < 0.05$) while the renal expression of 25-hydroxyvitamin D 24-hydroxylase was not different among groups.

Discussion

A recent study reported that high blood pressure is associated with an increase in the risk of bone loss [29]; this has led to an increase in interest in evaluating the effects of therapeutic agents for treatment of cardiovascular diseases on bone health and their potential use in the intervention of bone diseases. In addition, angiotensin-converting enzyme inhibitors (ACEIs) are currently in wide use for the treatment of diabetes complications, including cardiovascular events [30]. Furthermore, osteoporosis is often associated with hyperglycemia in animals [27] and patients [31]. Therefore, it is important to assess the impact of ACEIs on bone metabolism in diabetic conditions, which in turn might induce the most common renal complication, diabetic nephropathy [26]. In the present study, we investigated the effects of captopril, one of the classical ACEIs, on bone and kidney in experimental type 2 diabetic mice model.

This study showed that treatment with captopril in db/db mice was able to attenuate diabetes-induced renal injury as demonstrated by the prevention of albuminuria and glomerulosclerosis, which are the main pathological hallmarks of diabetic nephropathy [5]. Renal damage of db/db mice was also attributed to a marked increase in the expression of profibrotic factors such as CTGF and VEGF, both of which are main regulators for glomerulosclerosis. The pathological changes in histomorphology and molecular responses of diabetic kidneys were virtually prevented by the treatment with captopril. Of note was that the protective effects on renal functions, including serum creatinine and urine albumin, were independent of

glycemic control, indicating a direct effect of captopril on the kidney rather than the result of affected pancreatic insulin production or glucose metabolism. The proposed pharmacological mechanism of captopril in improving type 2 diabetic nephropathy was attributed to its suppression of the production of ANG II, one vital pathological factor leading to the increased expression of profibrotic proteins, renal fibrosis and even renal failure [5, 32].

The nephroprotection of ACEI on type 2 diabetic mice in this study was consistent with previous studies performed on type 1 diabetic animal model [33, 34]. In clinical setting ACEI was usually applied in combination with ARB or calcium channel blocker to slow down the progression of chronic kidney disease [35-37], suggesting a convincible beneficial effect of ACEI on renal health. However, this study demonstrated the unexpected results about the detrimental effects of captopril on the bone of type 2 diabetic mice, an important finding of the potential side effects of captopril on worsening bone health.

Previously, most clinical studies demonstrated that patients treated with ACEI had an increased bone mineral density (BMD) and a reduced fracture risk [14-16]. Moreover, the protective effects of ACEI on bone in experimental animal models have been reported [10, 38-39]. For example, treatment of Tsukuba hypertensive mouse with enalapril improved osteoporosis [38]; treatment of ovariectomized rats with ACEI captopril increased trabecular bone area of lumbar vertebrae (L4) and improved biomechanical properties by increasing L5 break stress and elastic modulus [39]; while ACEI perindopril was capable of accelerating bone healing and remodeling in a

murine femur fracture model [10]. The above-mentioned clinical and animal studies indicated the protective effects of ACEI against bone injuries.

Our study showed that intragastrical (i.g.) administration of captopril (10 mg/kg) for 8 weeks increased urinary excretion of calcium and phosphorus and trabecular bone separation and decreased BMD, bone volume and trabecular bone number in db/db mice. Histological staining and reconstructed micro-architecture consistently showed the aggravating destructive effects of captopril on trabecular bone at the proximal metaphysis of tibia of db/db mice. Similar effects of captopril (10 mg/kg, i.g.) on bone were reported in normal male mice [40] and type 1 diabetic mice [24], and similarly, 10-week treatment of perindopril (3 mg/kg/day, i.g.) has been reported to significantly reduce BMD in the distal metaphysis of femur in mouse fracture model [10]. The administration of enalapril (0.4 mg/kg, i.p.) did not cause any significant changes in bone density, the ash and mineral content or morphometric parameters of the femur in female Wistar rats [41]. Another ACEI moexipril, when given alone at the oral dosage of 10 mg/kg, had no effect on the cancellous bone site in either OVX or sham-operated rats [42]. Thus, this study displayed the potential effects of captopril on accelerating the loss of in vivo minerals and the deteriorations of trabecular bone in type 2 diabetic mice. However, the potential dose-dependent effects of ACEI on bone tissue require further investigation.

The expression of RAS and kallikrein-kinin system (KKS) components in bone was studied to determine the involvement of the relevant factors in the regulation of captopril on bone metabolism. Captopril effectively decreased the expression of

renin/renin receptor, ANG II and its receptor AT1R as well as bradykinin receptor-2 (B2R), which was reported to be capable of decreasing osteoblastic differentiation with concomitant increase in osteoclastic maturation, and consequently stimulated bone resorption and reduced BMD [43]. Thus, this study suggested the inhibitive effects of captopril on bone RAS and KKS in db/db mice. These results appeared to be contradictory to the study in which captopril was reported to exert chondroprotective effects in a rat model of osteoarthritis through its suppressive effect on local RAS [44]. Thus, the suppressive effects on ACE/ANGII/AT1R pathway and bradykinin pathway were contradictory to the observed impairment of trabecular bone brought about by captopril. Thereafter, we evaluated the influence of captopril on the circulating level of mineral metabolism-regulating hormones and the expression of renal vitamin D-related proteins as well as the mRNA expression of regulators for bone metabolism in bone tissue of db/db mice.

Our results were in agreement with those reported previously [45] that showed serum parathyroid hormone (PTH) level and renal expression of calcium-binding protein 28-k (CaBP-28k) were increased while renal vitamin D receptor (VDR) expression was reduced in db/db mice. Interestingly, captopril reversed these pathological changes in the regulators involved in mineral metabolism but did not reduce the urinary calcium and phosphorus levels in db/db mice. The results suggested that the captopril-induced elevation of calcium and phosphorus in urine was potentially attributed to its destruction of bone tissue and was independent of its modulating effects on the mineral homeostasis system.

Our results revealed the stimulatory effects of captopril treatment on the process of osteoclastogenesis as demonstrated by the increase in osteoclast-covered bone surface (OcS/BS) and the induction of the expression of osteoclastic resorptive marker carbonic anhydrase II (CAII), which could act on CO_2 and H_2O to generate hydrogen ions that would be secreted extracellularly by H^+-ATPase in osteoclasts to dissolve the inorganic substances in bone [24, 28]. Thus, the increased OcS/BS and the up-regulation of CAII expression may account for the enhanced loss of minerals in urine in this study. In addition, the administration of captopril decreased the osteoblast-covered bone surface (ObS/BS) and slowed down the process of osteogenesis by down-regulating the expression of the osteoblastic markers, RUNX2 and type 1 collagen. These striking effects of captopril were in accordance with its action on type 1 diabetic mice [24], indicating a direct detrimental effect of ACEI captopril on bone tissue of diabetic mice. Our results strengthened the experimental evidences that explain the recently emerging observations in clinical studies where women who used ACEI continuously were reported to have increased bone loss both in total hip and femoral neck [19], and ACEI users were associated with increased bone loss in a study on American men with a large sample size [18] and in a cohort study of atomic bomb survivors in Japan [20].

In conclusion, the present study demonstrated the beneficial effects of ACEI captopril on diabetic nephropathy as demonstrated by the inhibition of albuminuria and glomerulosclerosis through down-regulating the expression of ANG II and profibrotic factors in db/db mice, while the inhibitory effects of captopril on RAS

components locally in bone and serum PTH level as well as the expression of renal vitamin D-related factors did not result in any improvement of bone injury induced by diabetes. The potential worsening of captopril on the bone of db/db mice may at least partially be attributed to its direct regulation of osteoclast and osteoblast. Therefore, our study suggests that caution is needed in the clinical use of captopril (even ACEI) for treatment of diabetic complications, especially for those with high risks of bone loss.

References

[1] Namazi S, Ardeshir-Rouhani-Fard S, Abedtash H (2011) The effect of renin angiotensin system on tamoxifen resistance. Med Hypotheses 77:152-155

[2] Lozano-Maneiro L, Puente-García A (2015) Renin-angiotensin-aldosterone system blockade in diabetic nephropathy. Present evidences. J Clin Med 4:1908-1937

[3] Skov J, Persson F, Frøkiær J, Christiansen JS (2014) Tissue renin-angiotensin systems: a unifying hypothesis of metabolic disease. Front Endocrinol (Lausanne) 5:23

[4] Zhang Z, Zhang Y, Ning G, Deb DK, Kong J, Li YC (2008) Combination therapy with AT1 receptor blocker and vitamin D analog markedly ameliorates diabetic nephropathy. Proc Natl Acad Sci USA 105:15896-15901

[5] Zhang Y, Deb DK, Kong J et al (2009) Long-term therapeutic effect of vitamin D analog Doxercalciferol on diabetic nephropathy: strong synergism with AT1 receptor antagonist. Am J Physiol Renal Physiol 297:F791-F801

[6] Koïtka A, Cao Z, Koh P et al (2010) Angiotensin II subtype 2 receptor blockade and deficiency attenuate the development of atherosclerosis in an apolipoprotein E-deficient mouse model of diabetes. Diabetologia 53:584-592

[7] Inaba S, Iwai M, Furuno M et al (2011) Role of angiotensin-converting enzyme 2 in cardiac hypertrophy induced by nitric oxide synthase inhibition. J Hypertens 29:2236-2245

[8] Nakai K, Kawato T, Morita T, et al (2013) Angiotensin II induces the production

of MMP-3 and MMP-13 through the MAPK signaling pathways via the AT(1) receptor in osteoblasts. Biochimie 95:922-933

[9] Izu Y, Mizoguchi F, Kawamata A et al (2009) Angiotensin II type 2 receptor blockade increases bone mass. J Biol Chem 284:4857-4864

[10] Garcia P, Schwenzer S, Slotta JE et al (2010) Inhibition of angiotensin-converting enzyme stimulates fracture healing and periosteal callus formation - role of a local renin-angiotensin system. Br J Pharmacol 159:1672-1680

[11] Schlienger RG, Kraenzlin ME, Jick SS, Meier CR (2004) Use of beta-blockers and risk of fractures. JAMA 292:1326-1332

[12] Pérez-Castrillón JL, Silva J, Justo I et al (2003) Effect of quinapril, quinapril-hydrochlorothiazide, and enalapril on the bone mass of hypertensive subjects: relationship with angiotensin converting enzyme polymorphisms. Am J Hypertens 16:453-459

[13] Lynn H, Kwok T, Wong SY, Woo J, Leung PC (2006) Angiotensin converting enzyme inhibitor use is associated with higher bone mineral density in elderly Chinese. Bone 38:584-588

[14] García-Testal A, Monzó A, Rabanaque G, González A, Romeu A (2006) Evolution of the bone mass of hypertense menopausal women in treatment with fosinopril. Med Clin (Barc) 127:692-694

[15] Rejnmark L, Vestergaard P, Mosekilde L (2006) Treatment with beta-blockers, ACE inhibitors, and calcium-channel blockers is associated with a reduced fracture risk: a nationwide case-control study. J Hypertens 24:581-589

[16] Ghosh M, Majumdar SR (2014) Antihypertensive medications, bone mineral density, and fractures: a review of old cardiac drugs that provides new insights into osteoporosis. Endocrine 46:397-405

[17] Solomon DH, Mogun H, Garneau K, Fischer MA (2011) Risk of fractures in older adults using antihypertensive medications. J Bone Miner Res 26:1561-1567

[18] Kwok T, Leung J, Zhang YF et al (2012) Does the use of ACE inhibitors or angiotensin receptor blockers affect bone loss in older men? Osteoporos Int 23:2159-2167

[19] Zhang YF, Qin L, Leung PC, Kwok TC (2012) The effect of angiotensin-converting enzyme inhibitor use on bone loss in elderly Chinese. J Bone Miner Metab 30:666-673

[20] Masunari N, Fujiwara S, Nakata Y, Furukawa K, Kasagi F (2008) Effect of angiotensin converting enzyme inhibitor and benzodiazepine intake on bone loss in older Japanese. Hiroshima J Med Sci 57:17-25

[21] Shaw JE, Sicree RA, Zimmet PZ (2010) Global estimates of the prevalence of diabetes for 2010 and 2030. Diabetes Res Clin Pract 87:4-14

[22] Roy B (2013) Biomolecular basis of the role of diabetes mellitus in osteoporosis and bone fractures. World J Diabetes 4:101-113

[23] Zhang Y, Diao TY, Gu SS et al (2014) Effects of angiotensin II type 1 receptor blocker on bones in mice with type 1 diabetes induced by streptozotocin. J Renin Angiotensin Aldosterone Syst 15:218-227

[24] Diao TY, Pan H, Gu SS et al (2014) Effects of angiotensin-converting enzyme

inhibitor, captopril, on bone of mice with streptozotocin-induced type 1 diabetes. J Bone Miner Metab 32:261-270

[25] Zhang Y, Wang Y, Chen Y et al (2012) Inhibition of renin activity by aliskiren ameliorates diabetic nephropathy in type 1 diabetes mouse model. J Diabetes Mellitus 2:353-360

[26] Zhang Z, Sun L, Wang Y et al (2008) Renoprotective role of the vitamin D receptor in diabetic nephropathy. Kidney Int 73:163-171

[27] Zhang Y, Papasian CJ, Deng H (2011) Alteration of vitamin D metabolic enzyme expression and calcium transporters abundance in kidney involved in type 1 diabetes-induced bone loss. Osteoporos Int 22:1781-1788

[28] Zhang Y, Dong XL, Leung PC, Wong MS (2009) Differential mRNA expression profiles in proximal tibia of aged rats in response to ovariectomy and low-Ca diet. Bone 44:46-52

[29] Cappuccio FP, Meilahn E, Zmuda JM, Cauley JA (1999) High blood pressure and bone-mineral loss in elderly white women: a prospective study. Study of Osteoporotic Fractures Research Group. Lancet 354:971-975

[30] Cheng J, Zhang W, Zhang X et al (2014) Effect of angiotensin-converting enzyme inhibitors and angiotensin II receptor blockers on all-cause mortality, cardiovascular deaths, and cardiovascular events in patients with diabetes mellitus: a meta-analysis. JAMA Intern Med 174:773-785

[31] Hofbauer LC, Brueck CC, Singh SK, Dobnig H (2007) Osteoporosis in patients with diabetes mellitus. J Bone Miner Res 22:1317-1328

[32] Zhang Y, Kong J, Deb DK, Chang A, Li YC (2010) Vitamin D receptor attenuates renal fibrosis by suppressing the renin-angiotensin system. J Am Soc Nephrol 21:966-973

[33] Ertürküner SP, Başar M, Tunçdemir M, Seçkin İ (2014) The comparative effects of perindopril and catechin on mesangial matrix and podocytes in the streptozotocin induced diabetic rats. Pharmacol Rep 66:279-287

[34] Huang H, Hu L, Lin J, Zhu X, Cui W, Xu W (2015) Effect of fosinopril on chemerin and VEGF expression in diabetic nephropathy rats. Int J Clin Exp Pathol 8:11470-11474

[35] Nakamura A, Shikata K, Nakatou T et al (2013) Combination therapy with an angiotensin-converting-enzyme inhibitor and an angiotensin II receptor antagonist ameliorates microinflammation and oxidative stress in patients with diabetic nephropathy. J Diabetes Investig 4:195-201

[36] Ren F, Tang L, Cai Y et al (2015) Meta-analysis: the efficacy and safety of combined treatment with ARB and ACEI on diabetic nephropathy. Ren Fail 37:548-561

[37] Huang RS, Cheng YM, Zeng XX, Kim S, Fu P (2016) Renoprotective effect of the combination of renin-angiotensin system inhibitor and calcium channel blocker in patients with hypertension and chronic kidney disease. Chin Med J (Engl) 129:562-569

[38] Asaba Y, Ito M, Fumoto T et al (2009) Activation of renin-angiotensin system induces osteoporosis independently of hypertension. J Bone Miner Res 24:241-250

[39] Liu YY, Yao WM, Wu T, Xu BL, Chen F, Cui L (2011) Captopril improves osteopenia in ovariectomized rats and promotes bone formation in osteoblasts. J Bone Miner Metab 29:149-158

[40] Liu JX, Wang L, Zhang Y (2015) Involvement of renin-angiotensin system in damage of angiotensin-converting enzyme inhibitor captopril on bone of normal mice. Biol Pharm Bull 38:869-875

[41] Broulík PD, Tesar V, Zima T, Jirsa M (2001) Impact of antihypertensive therapy on the skeleton: effects of enalapril and AT1 receptor antagonist losartan in female rats. Physiol Res 50:353-358

[42] Stimpel M, Jee WS, Ma Y, Yamamoto N, Chen Y (1995) Impact of antihypertensive therapy on postmenopausal osteoporosis: effects of the angiotensin converting enzyme inhibitor moexipril, 17beta-estradiol and their combination on the ovariectomy-induced cancellous bone loss in young rats. J Hypertens 13:1852-1856

[43] Srivastava S, Sharma K, Kumar N, Roy P (2014) Bradykinin regulates osteoblast differentiation by Akt/ERK/NFκB signaling axis. J Cell Physiol 229:2088-2105

[44] Tang Y, Hu XP, Lu XW (2015) Captopril, an angiotensin-converting enzyme inhibitor, possesses chondroprotective efficacy in a rat model of osteoarthritis through suppression local renin-angiotensin system. Int J Clin Exp Med 8:12584-12592

[45] Wang Y, Zhou J, Minto AW et al (2006) Altered vitamin D metabolism in type II diabetic mouse glomeruli may provide protection from diabetic nephropathy. Kidney Int 70:882-891

Acknowledgements

This work was supported by the Program of Innovative Research Team from Ministry of Science and Technology of P.R.China (2015RA4002), the Key Laboratory of Theory and Therapy of Muscles and Bones, Ministry of Education (<2009> No. 98), Innovative Research Team in University (PCSIRT, IRT1270), the National Natural Science Foundation of China (81573992, 81403239, 81220108027) and Longhua Medical Innovation Team Program (LYCX-01) as well as Natural Science Foundation of Shanghai.

Competing financial interests

The authors declare no competing financial interests.

Table 1 Effect of captopril on calcium and phosphorus in serum and urine of db/db mice

	S-Ca (mg/dl)	S-P (mg/dl)	U-Ca/Cr (mg/mg)	U-P/Cr (mg/mg)
db/+	10.07 ± 0.10	6.71 ± 0.21	0.083 ± 0.011	0.522 ± 0.069
db/db	10.31 ± 0.17	7.05 ± 0.30	0.072 ± 0.016	0.404 ± 0.075
Captopril	10.72 ± 0.32	7.93 ± 0.22*	0.449 ± 0.118#	1.556 ± 0.373#

Values are expressed as means ± SEM, n = 10-12 in either group. * $P < 0.05$, vs. db/+ group; # $P < 0.05$, vs. db/db group. S, serum; U, urine; Ca, calcium; Cr, creatinine; P, phosphorus.

Table 2 Effect of captopril on biomarkers in serum of db/db mice

	Testosterone (ng/ml)	PTH (pg/ml)	FGF-23 (pg/ml)
db/+	0.389 ± 0.128	116.8 ± 21.2	334.0 ± 30.1
db/db	0.298 ± 0.129	173.7 ± 10.1*	181.1 ± 23.2**
Captopril	0.291 ± 0.054	104.7 ± 12.5##	180.5 ± 13.5

Values are expressed as means ± SEM, n = 10~12 in either group. * $P < 0.05$, ** $P < 0.01$, vs. db/+ group; ## $P < 0.01$, vs. db/db group. PTH, parathyroid hormone; FGF-23, fibroblast growth factor-23.

Table 3 Effect of captopril on bone parameters at the proximal tibial metaphysis of db/db mice measured by quantitative microcomputed tomography

	db/+	db/db	Captopril
BV/TV	0.383 ± 0.038	0.133 ± 0.005***	0.095 ± 0.006##
Conn.D (1/mm^3)	487.4 ± 58.5	122.1 ± 27.8***	62.5 ± 9.6
SMI	1.06 ± 0.44	2.33 ± 0.10*	2.29 ± 0.12
Tb.N (1/mm)	6.92 ± 0.30	3.05 ± 0.09***	2.18 ± 0.13###
Tb.Th (μm)	54.9 ± 3.3	41.7 ± 0.8**	41.7 ± 0.8
Tb.Sp (μm)	90.7 ± 9.2	286.8 ± 10.7***	424.1 ± 29.5##
BMD/TV (mg HA/ccm)	276.5 ± 20.1	118.2 ± 8.3***	73.7 ± 5.8##
BS/BV (1/mm)	36.9 ± 1.9	48.1 ± 1.0***	48.1 ± 0.9
DA	1.78 ± 0.05	1.94 ± 0.07	1.98 ± 0.09

Values are expressed as means ± SEM, n = 10~12 in either group. * P < 0.05, ** P < 0.01, *** P < 0.001, vs. db/+ group; ## P < 0.01, ### P < 0.001, vs. db/db group. BV/TV, bone volume over total volume; Conn. D, connectivity density; SMI, structure model index; Tb.N, trabecular bone number; Tb.Th, trabecular bone thickness; Tb.Sp, trabecular bone separation; BMD/TV, bone mineral density over total volume; BS/BV, bone surface over bone volume; DA, degree of anisotropy.

Figure legends

Fig.1 Effect of captopril on body weight, fasting blood glucose, serum creatinine and urinary albumin of db/db mice. A, body weight; B, fasting blood glucose level; C, serum creatinine; D, urinary albumin to creatinine ratio (ACR, μg/mg). Values are expressed as means ± SEM, n = 10-12. * $P < 0.05$, *** $P < 0.001$, vs. db/+ group; # $P < 0.05$, ## $P < 0.01$, vs. db/db group.

Fig.2 Effect of captopril on glomerulosclerosis, the protein expression of ANG II and the mRNA expression of profibrotic cytokines in kidney. A, representative glomerular morphology from periodic acid-Schiff (PAS) staining. Note the severe glomerular sclerosis in the kidney of db/db group and the improvement after the captopril treatment. B, semiquantitative glomerulosclerotic score. C, protein expression of ANG II in kidney and the densitometric quantification (D). E, mRNA expression of connective tissue growth factor (*CTGF*) and vascular endothelial growth factor (*VEGF*) in the kidney and the densitometric quantification (F). Values are expressed as means ± SEM, n = 10-12. * $P < 0.05$, ** $P < 0.01$, *** $P < 0.001$, vs. db/+ group; # $P < 0.05$, ### $P < 0.001$, vs. db/db group.

Fig.3 Histological images of the proximal tibial metaphysis, measured by Safranin O staining (A, Magnification, ×50) and Masson-Trichrome staining (B, Magnification, ×100), in the control group and the db/db group treated with vehicle or captopril for 8

weeks. The trabecular bone area over total area (BA/TA, C) and the width of the cartilage overlying the epiphyseal plate (D) were quantified. Values are expressed as means ± SEM, n = 10. * $P < 0.05$, ** $P < 0.01$, vs. db/+ group; ## $P < 0.01$, vs. db/db group.

Fig.4 Representative microcomputed tomography 3-dimensional images of the proximal metaphysis of tibia in the control group and the db/db group treated with vehicle or captopril for 8 weeks.

Fig.5 mRNA expression of RAS components in femur (A), and the densitometric quantification of the mRNA expression levels, which are expressed as a ratio to the expression of *GAPDH* (B). *Renin-R*, renin receptor; *AT1R*, angiotensin II type 1 receptor. Values are expressed as means ± SEM, n = 10-12. * $P < 0.05$, ** $P < 0.01$, vs. db/+ group; # $P < 0.05$, ## $P < 0.01$, vs. db/db group.

Fig.6 Protein expression of renin, angiotensin II (ANG II), ANG II type 1 receptor (AT1R), bradykinin receptor-1 (B1R) and bradykinin receptor-2 (B2R) in femur (A) and the densitometric quantification of the protein expression levels, which are expressed as a ratio to the expression of β-actin (B). Values are expressed as means ± SEM, n = 10-12. * $P < 0.05$, ** $P < 0.01$, *** $P < 0.001$, vs. db/+ group; # $P < 0.05$, ## $P < 0.01$, vs. db/db group.

Fig.7 TRAP staining for osteoclasts and modified Gomori staining for osteoblasts in the proximal metaphysis of tibia. A, representative images (osteoclasts shown by arrows in blue, Magnification ×400). B, osteoclast-covered bone surface (OcS/BS). C, representative images (osteoblasts shown by black staining, Magnification ×200). D, osteoblast-covered bone surface (ObS/BS). Values are expressed as means ± SEM, *n* = 10. * *P* < 0.05, ***P* < 0.01, vs. db/+ group; # *P* < 0.05, vs. db/db group.

Fig.8 mRNA expression in femur (A) of type 1 collagen (*COL*), runt-related transcription factor 2 (*RUNX2*), carbonic anhydrase II (*CAII*) and matrix metalloproteinase (*MMP*)-9 and the densitometric quantification (B) of the mRNA expression levels, which are expressed as a ratio to the expression of GAPDH. Values are expressed as means ± SEM, *n* = 10-12. * *P* < 0.05, ***P* < 0.01, vs. db/+ group; # *P* < 0.05, ## *P* < 0.01, vs. db/db group.

Fig.9 Protein expression of 25-hydroxyvitamin D-24 hydroxylase (24-OHase), calcium-binding protein 28-k (CaBP-28K), and vitamin D receptor (VDR) in the kidney (A) and the densitometric quantification of the protein expression levels, which are expressed as a ratio to the expression of β-actin (B). Values are expressed as means ± SEM, n = 10-12. ** *P* < 0.01, *** *P* < 0.001, vs. db/+ group; # *P* < 0.05, ### *P* < 0.001, vs. db/db group.

Figure 1

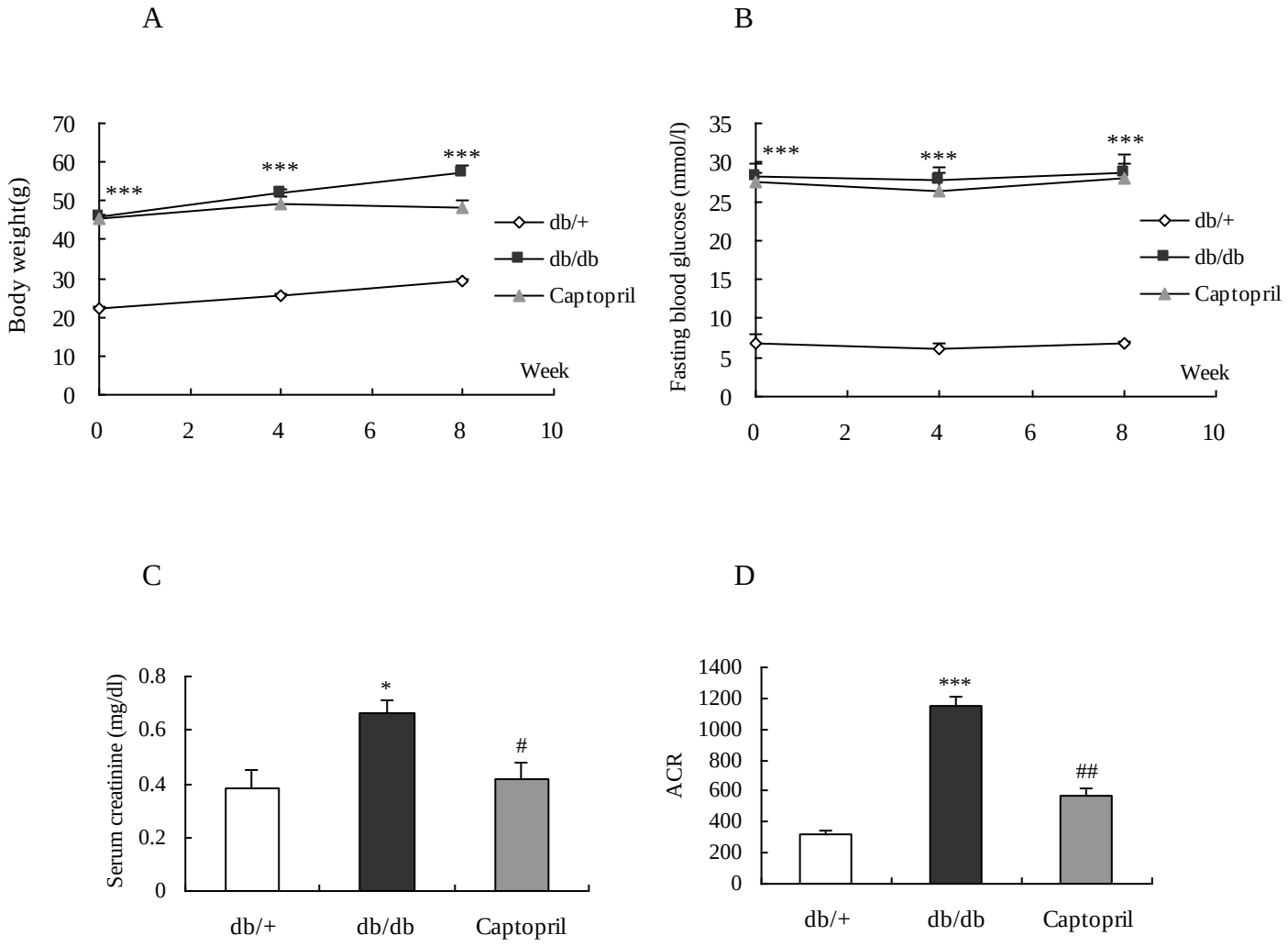
A
B
C
D
Body weight(g)
Week
db/+
db/db
Captopril
***
Fasting blood glucose (mmol/l)
Serum creatinine (mg/dl)
*
#
ACR
##
db/+
db/db
Captopril

Figure 2

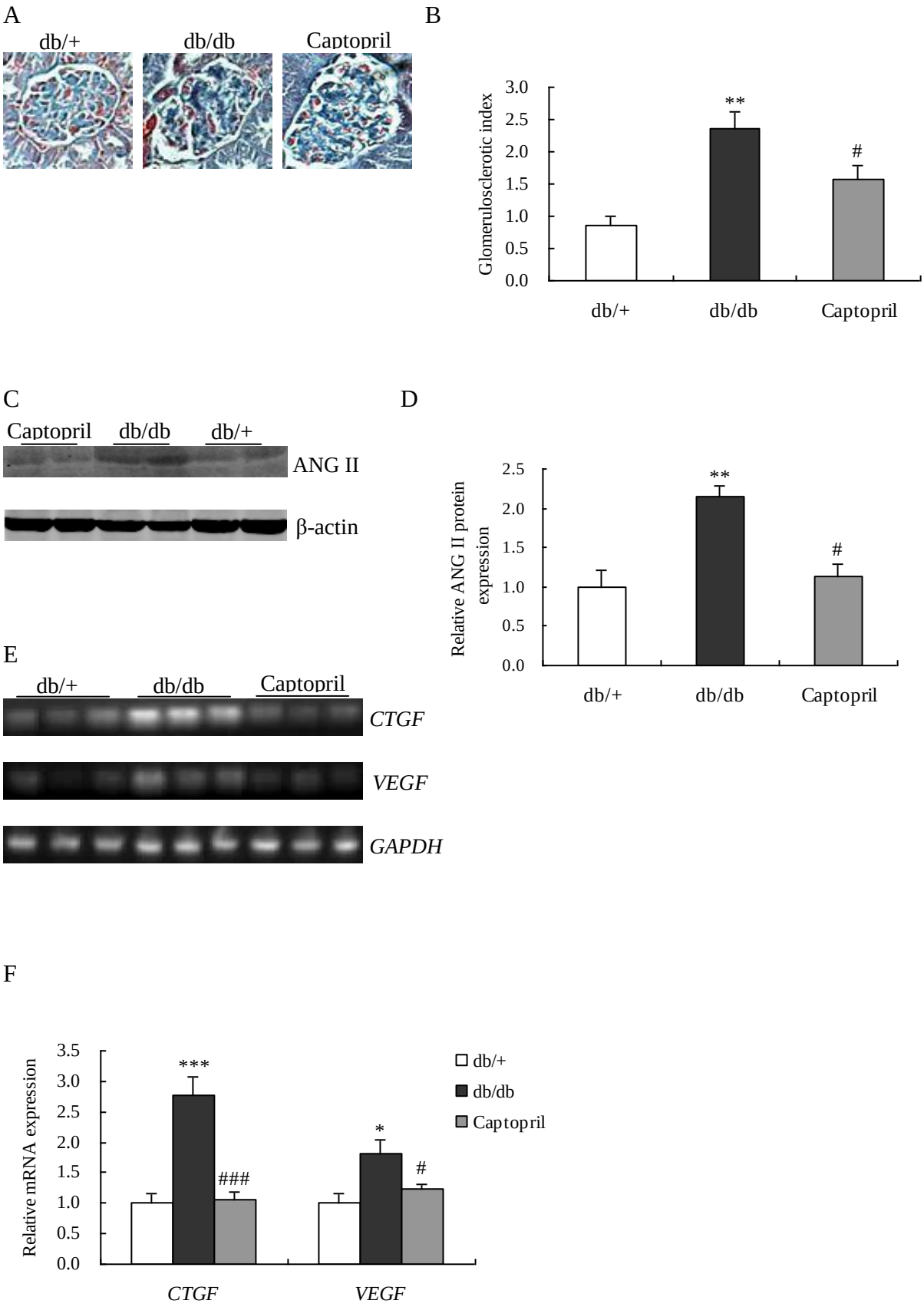
A
db/+
db/db
Captopril
B
Glomerulosclerotic index
3.0
2.5
2.0
1.5
1.0
0.5
0.0
**
#
db/+
db/db
Captopril
C
Captopril
db/db
db/+
ANG II
β-actin
D
Relative ANG II protein expression
2.5
2.0
1.5
1.0
0.5
0.0
**
#
db/+
db/db
Captopril
E
db/+
db/db
Captopril
CTGF
VEGF
GAPDH
F
Relative mRNA expression
3.5
3.0
2.5
2.0
1.5
1.0
0.5
0.0
***
###
*
#
db/+
db/db
Captopril
CTGF
VEGF

Figure 3

A

B

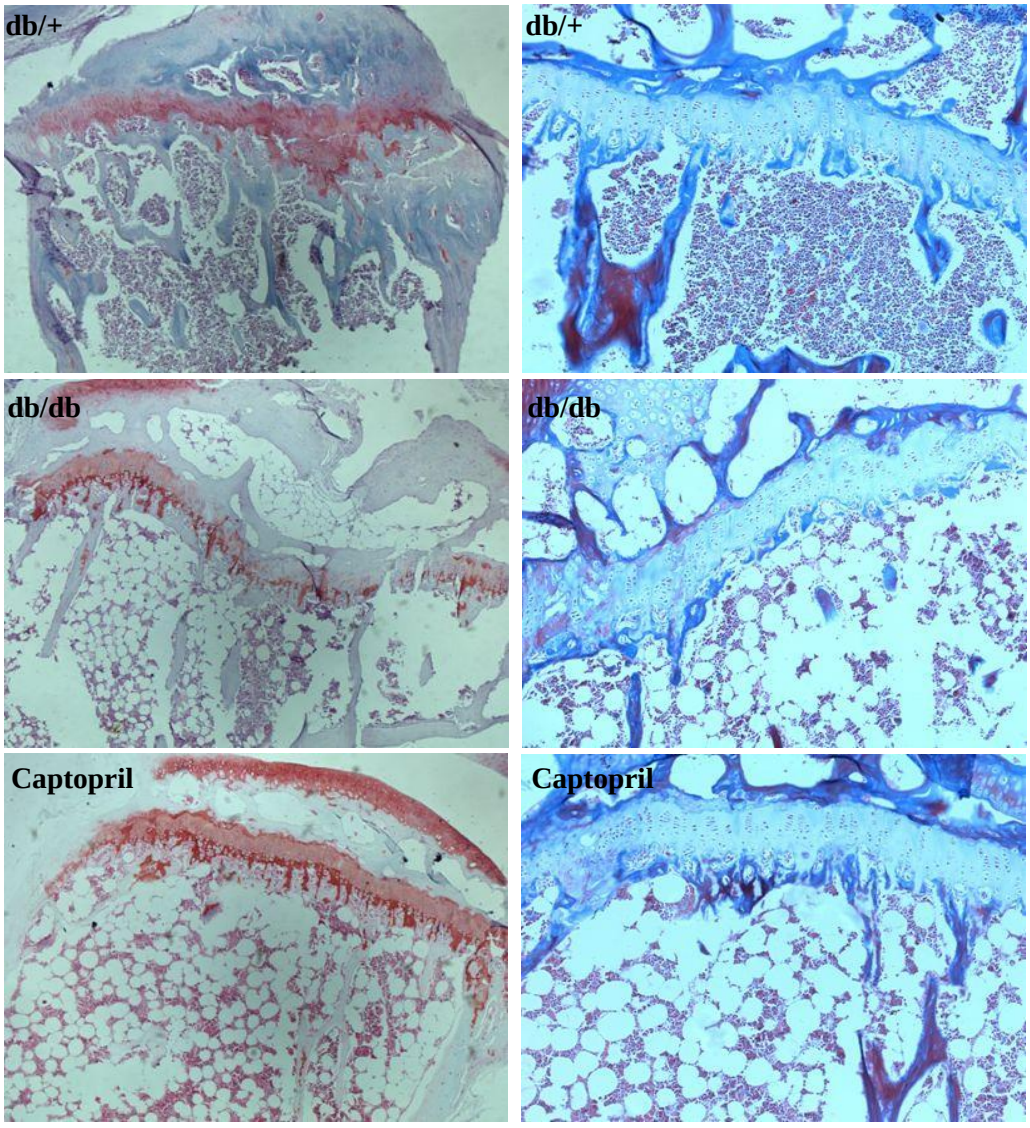
db/+
db/+
db/db
db/db
Captopril
Captopril

C

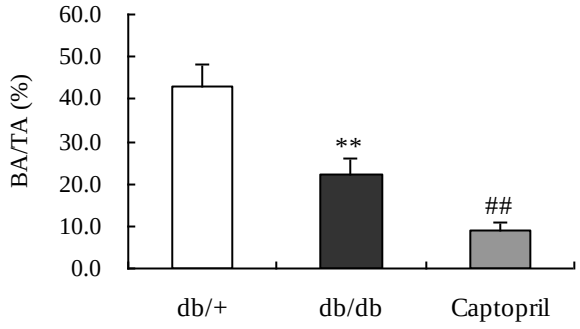
60.0
50.0
40.0
30.0
20.0
10.0
0.0
BA/TA (%)
**
##
db/+
db/db
Captopril

D

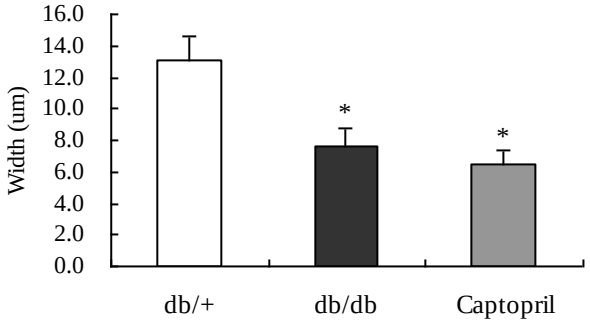

Figure 4

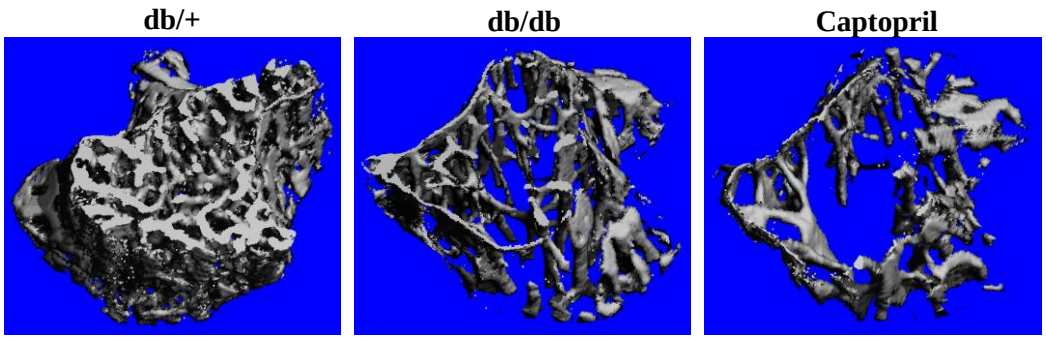

Figure 5

A

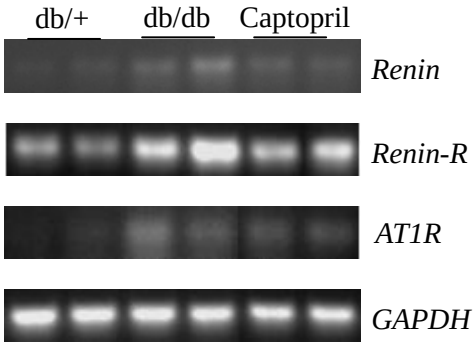
db/+
db/db
Captopril
Renin
Renin-R
AT1R
GAPDH

B

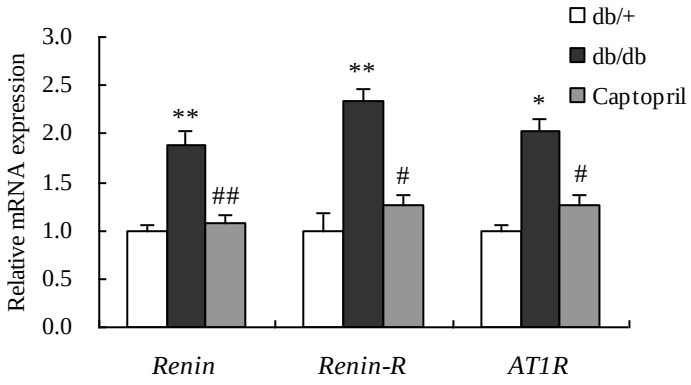
db/+
db/db
Captopril
Relative mRNA expression
3.0
2.5
2.0
1.5
1.0
0.5
0.0
**
##
**
#
*
#
Renin
Renin-R
AT1R

Figure 6

A

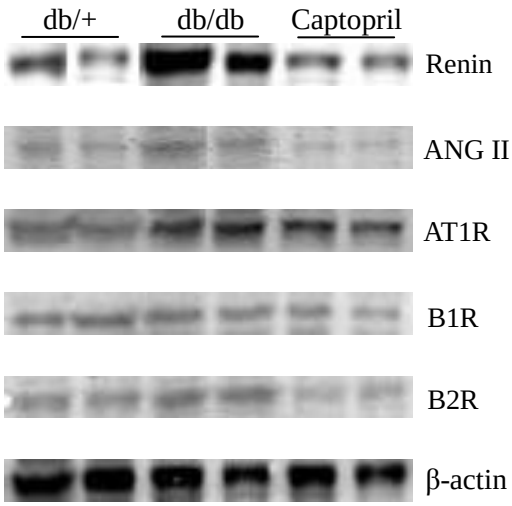
db/+
db/db
Captopril
Renin
ANG II
AT1R
B1R
B2R
β-actin

B

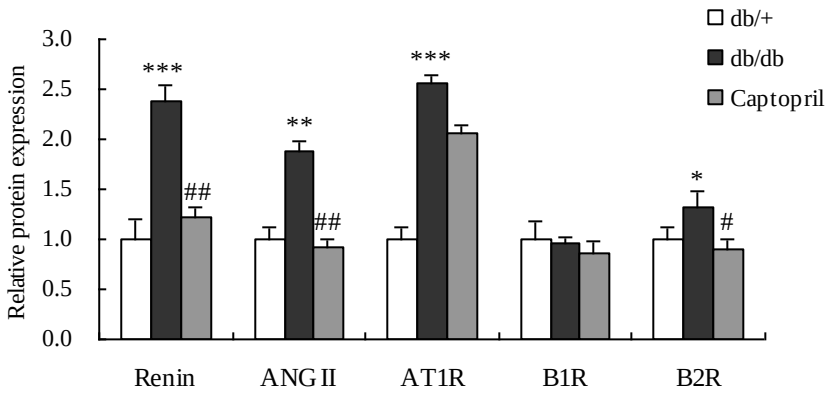
db/+
db/db
Captopril
Relative protein expression
3.0
2.5
2.0
1.5
1.0
0.5
0.0
***
**
***
*
##
##
#
Renin
ANG II
AT1R
B1R
B2R

Figure 7

A

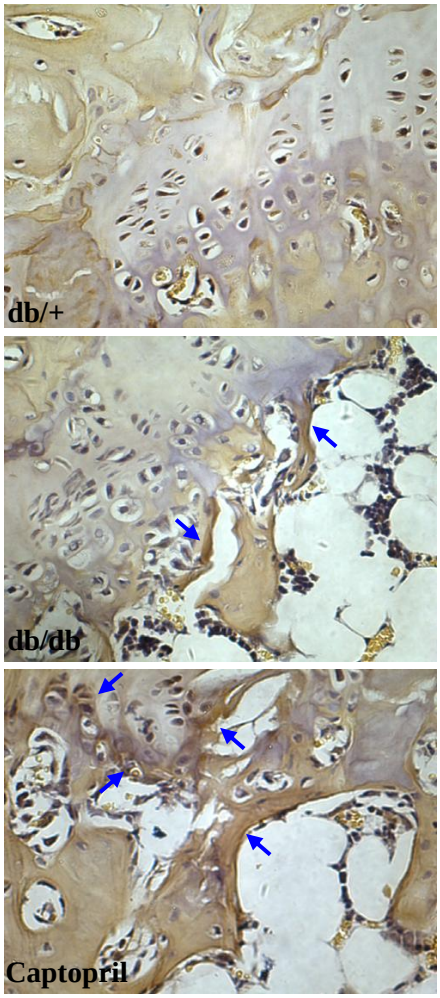
db/+
db/db
Captopril

B

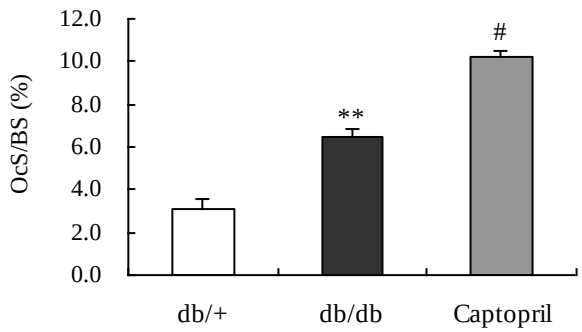
OcS/BS (%)
12.0
10.0
8.0
6.0
4.0
2.0
0.0
**
#
db/+
db/db
Captopril

C

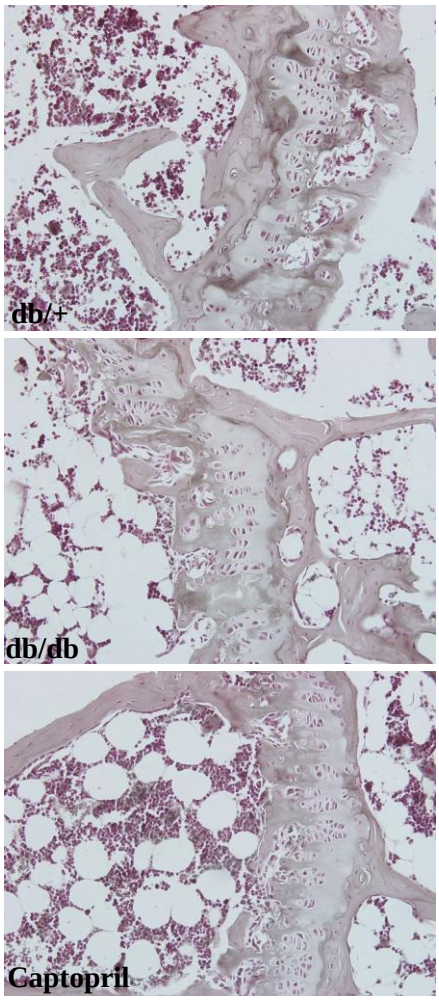
db/+
db/db
Captopril

D

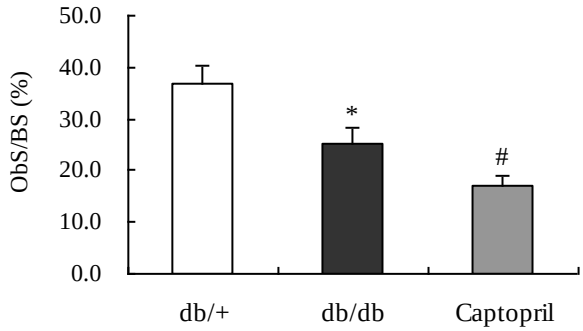
50.0
40.0
30.0
20.0
10.0
0.0
ObS/BS (%)
*
#
db/+
db/db
Captopril

Figure 8

A

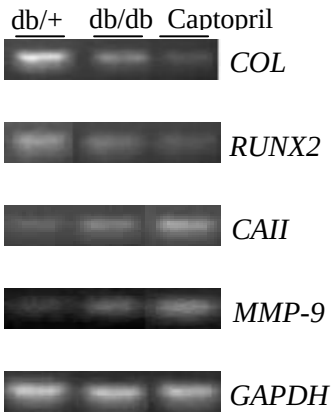
db/+
db/db
Captopril
COL
RUNX2
CAII
MMP-9
GAPDH

B

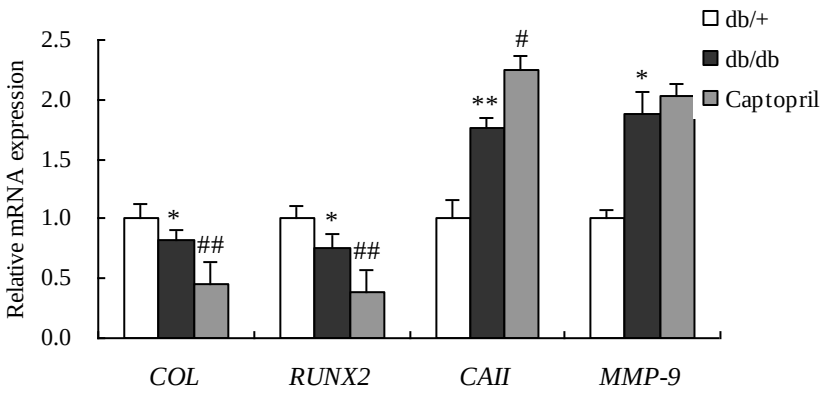
db/+
db/db
Captopril
Relative mRNA expression
2.5
2.0
1.5
1.0
0.5
0.0
*
##
*
##
**
#
*
COL
RUNX2
CAII
MMP-9

Figure 9

A

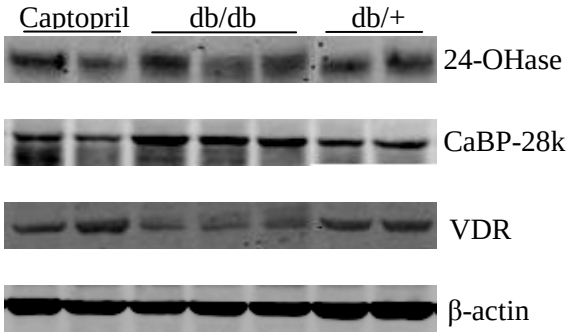
Captopril
db/db
db/+
24-OHase
CaBP-28k
VDR
β-actin

B

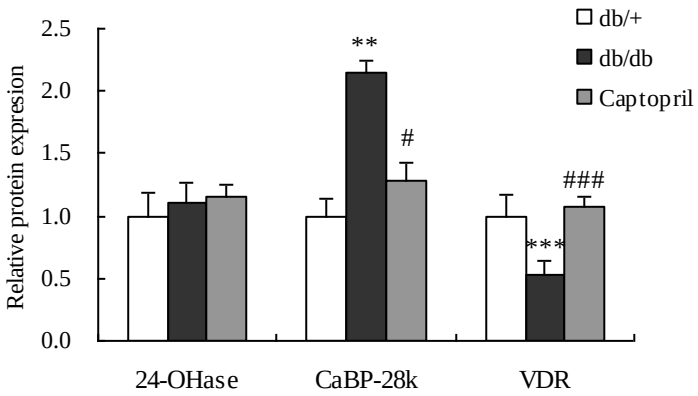
db/+
db/db
Captopril
Relative protein expresion
2.5
2.0
1.5
1.0
0.5
0.0
**
#
###
***
24-OHase
CaBP-28k
VDR